

Geologic and Geotechnical Factors Controlling Incipient Slope Instability at a Gravel Quarry, Livermore Basin, California



PHILIP L. JOHNSON¹
PATRICK O. SHIRES
TIMOTHY P. SNEDDON

Cotton, Shires and Associates, 330 Village Lane, Los Gatos, CA 95030

Key Terms: *Slope Instability, Gravel Quarry, Landslide, Stratigraphy*

ABSTRACT

Mine pit slopes at Arroyo del Valle Quarry in the Livermore Basin of northern California expose late Quaternary sandy gravel. In the deep subsurface, the gravel unconformably overlies gently folded lacustrine sediments. Within the lacustrine sediments, a bed of sheared, unoxidized clay overlies a marl bed, forming a distinctive marker bed couplet. Structure contours on this marker bed show an anticline and a syncline in the vicinity of the quarry. These northwest-striking folds are aligned parallel to regional Quaternary fold and thrust belt structures. Where the marker bed dips toward the pit, slope inclinometers consistently deflected toward the pit at the depth of the unoxidized clay. Where the marker bed dips away from the quarry pit, no slope inclinometer deflections were recorded. Thus, slope instability was controlled by the site stratigraphy, geologic structure, and the location of quarry slopes relative to that geologic structure. High pore-water pressures within the unoxidized clay also contributed to slope instability. Shearing of the unoxidized clay occurred prior to excavation of the quarry pit, and the resulting low residual strength of this high-plasticity clay made it particularly vulnerable to incipient landsliding when lateral confinement was removed during excavation of the quarry pit. Analysis of the critical region between the quarry pit and the anticline axis showed that the static factor of safety remained below 1.5. Seismic displacement analyses indicated that moderate to large displacements would be anticipated. Thus, depressurization wells and an earth-fill buttress were designed and implemented to mitigate deep-seated slope instability.

INTRODUCTION

Mine slope stability has been studied extensively at sites at which mine slopes expose fractured rock, and the application of rock mechanics to the study of mine slopes has aided in the design of stable slopes for long-term mine reclamation and short-term slope stability during mining operations (Hoek and Karzulovik, 2000; Wyllie and Mah, 2004). In some cases, rock slopes in open pit mines have experienced large, fast-moving failures (Pankow et al., 2014) that present significant challenges to mining operations.

By contrast, the stability of gravel quarry slopes that expose Quaternary sediments has received less attention. However, as mining of aggregate resources from basins within large metropolitan areas continues and urban development encloses the mined lands, the stability of gravel quarry slopes has become a significant concern (Doughton, 2009). Modern mining methods have allowed extraction of aggregate and other resources to significant depths within sedimentary basins, and dewatering systems have allowed mining of aggregate well below the groundwater table. Thus, relatively deep quarry excavations may be found locally within populated regions. Where the mine pits expose coarse granular materials, pit slope stability should be a simple function of slope angle, slope height, and (relatively high) material strengths. However, where the geologic conditions are more complex, slope stability may be more challenging to achieve.

Arroyo del Valle Quarry is a gravel quarry located in the Livermore Basin of northern California (Figure 1). Sand and gravel have been mined extensively in the Livermore Basin since the early 20th century for use as aggregate (Goldman, 1964; Dupras, 1999). The quarry is the easternmost of a series of gravel pits within the southern portion of the basin. Once mining of an individual pit is completed and dewatering systems are shut down, the pits are allowed to flood slowly by groundwater seepage, becoming artificial

¹Corresponding author email: pjohnson@cottonshires.com.

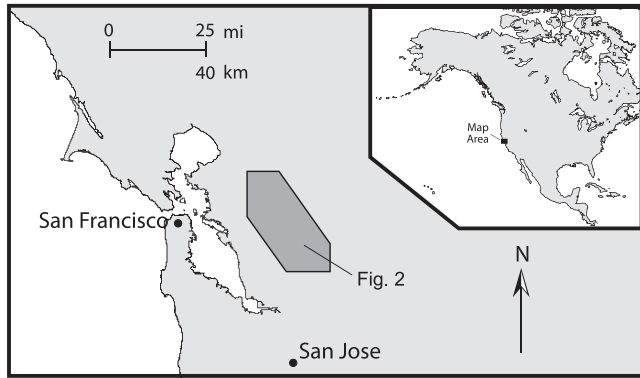


Figure 1. Location map for the Livermore Basin and surrounding uplifts.

lakes. Suburban residential development within the Livermore Basin has grown extensively since the 1980s and has approached the margins of the former gravel pits. At Arroyo del Valle Quarry, residential development extends up to the northeast boundary of the quarry property, currently within approximately 125 ft of the quarry pit.

The Arroyo del Valle Quarry is located within a geologically complex setting that may appear to be relatively simple at the surface and within the shallow subsurface. The mine pit slopes expose dense sandy gravel that appears to remain stable at slope inclinations of 2H:1V (26.6°) or greater. However, slope inclinometers installed around the mine pit have recorded deflections at depth, below the gravel exposed in the quarry pit. In this article, the unique site stratigraphy, geologic structure, and hydrogeology found in the subsurface at Arroyo del Valle Quarry and the impact of this unique geology on the stability of the quarry slopes are described. In addition, analyses of static and seismic slope stability and the design of mitigation measures that were implemented to achieve long-term stability of the former quarry pit slopes are described.

GEOLOGIC SETTING

The roughly east-west-trending late Quaternary Livermore Basin (Figure 2) is filled with non-marine clastic sediments (Barlock, 1989; Helley and Graymer, 1997). During Miocene to early Pleistocene time, the ancestral Livermore Basin (Unruh et al., 1997) extended beyond the limits of the late Quaternary basin, and upper Miocene to lower Pleistocene sedimentary rocks of the Sycamore, Tassajara, and Livermore formations are exposed in the hills that surround the late Quaternary basin (Andersen et al., 1995). The sediments that fill the late Quaternary Livermore Basin consist of Pleistocene to Holocene alluvial fan,

terrace, and floodplain deposits that overlie the Livermore Formation (Helley and Graymer, 1997). Early work by the California Department of Water Resources (CDWR, 1974) included characterization of the alluvial aquifers of the late Quaternary Livermore Basin. These aquifers contain a large volume of coarse-grained sediment that was derived from the Diablo Range to the south and transported by alluvial processes northward into the basin. Fine-grained lacustrine sediments form aquitards that cap the aquifer units. Ehman et al. (2004) interpreted electric logs and cuttings logs from 37 water wells in the central portion of the basin (north of Arroyo del Valle Quarry) and used sequence stratigraphic methods to characterize the aquifer stratigraphy and to identify several depositional sequences that are bounded by unconformities.

Crane (1995, 2007) mapped the northern, eastern, and western boundaries of the late Quaternary basin as faults that bound the hills that surround the basin. He interpreted the northern boundary of the basin as a southwest vergent thrust fault that bounds the Mount Diablo region (Figure 2), while complex thrust and strike slip faulting characterize the hills to the east and west. Thus, the late Quaternary Livermore Basin is flanked by faulted uplifts that expose tilted and folded Miocene to lower Pleistocene rocks.

Sawyer and Unruh (2004) identified a southwest vergent fold and thrust belt, the Mount Diablo Fold and Thrust Belt (MDFTB), that encompasses the Mount Diablo region and the Livermore Basin. Compressional deformation of the MDFTB has been attributed to a restraining left stepover between the right lateral Greenville and Concord faults (Unruh and Lettis, 1998). Unruh et al. (2007) view the Livermore Basin as deformed by active folding and southwest vergent thrust faulting behind the leading edge of the MDFTB, which extends as far southwest as the Verona and Williams faults (Figure 2). Several northwest striking and actively growing folds were identified within the basin and surrounding hills (Sawyer and Unruh, 2004). Thus, compressional tectonics of the MDFTB appear to be responsible for local deformation of Livermore Basin sediments.

GEOLOGY OF THE ARROYO DEL VALLE QUARRY AREA

Site Geomorphology

The geomorphology of the Arroyo del Valle Quarry site and surrounding area was mapped using stereo pairs of historic aerial photographs that pre-date the excavation of the quarry (Figure 3). The geomorphic

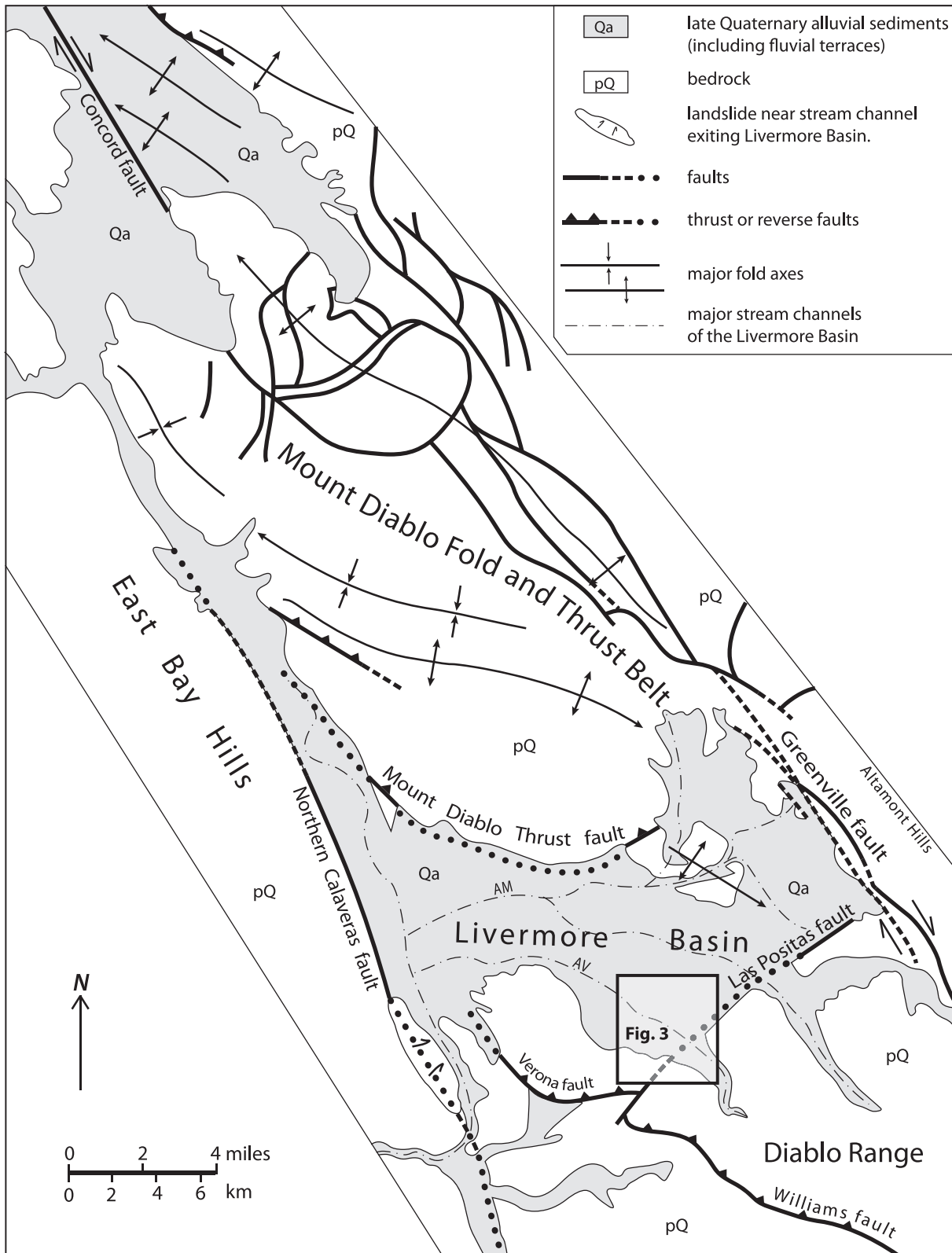


Figure 2. Simplified map of the Livermore Basin and major mapped faults, modified from Wagner et al. (1990). The labeled primary stream channels within the basin are Arroyo del Valle (AV) and Arroyo Mocho (AM).

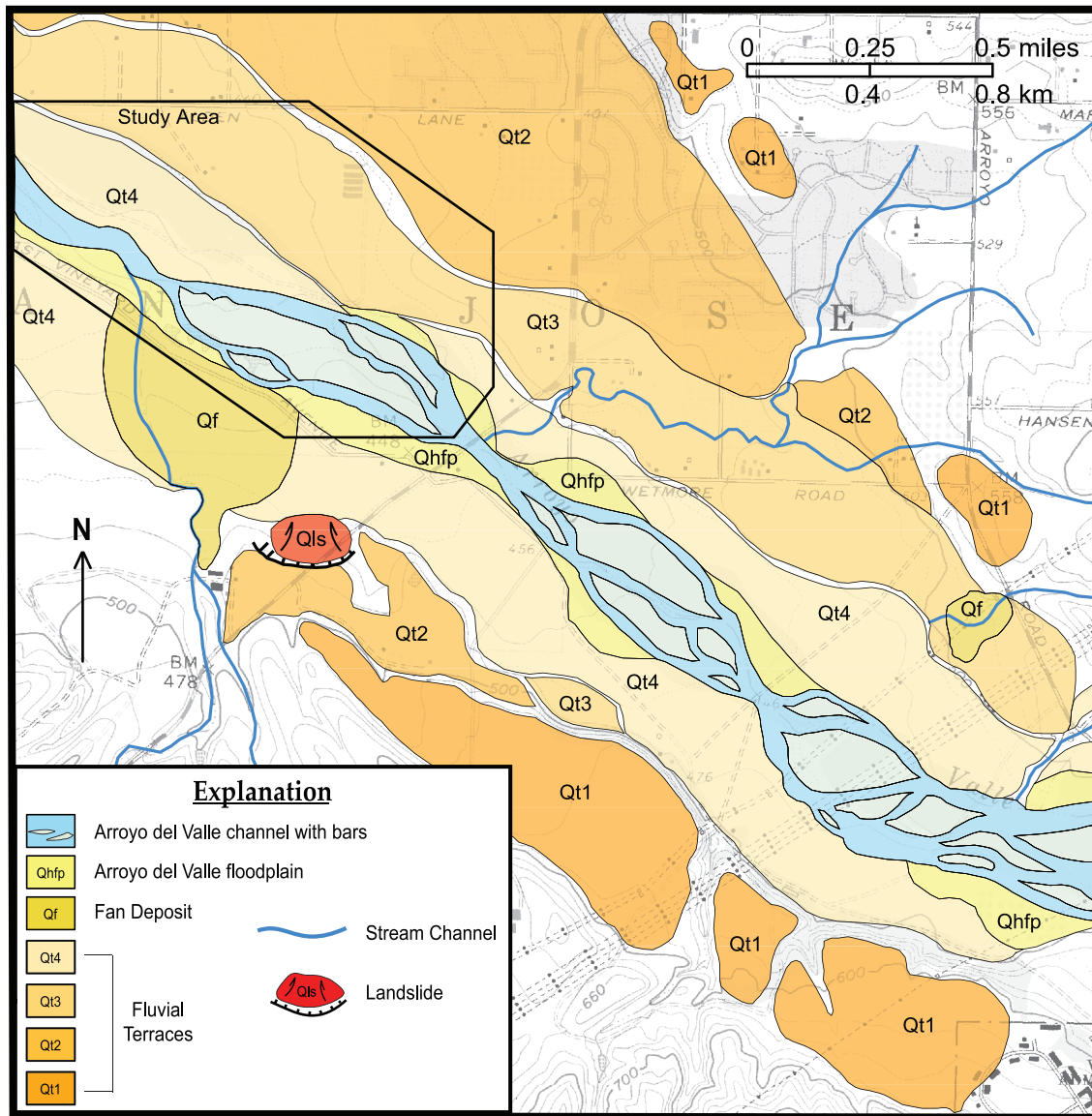


Figure 3. Photogeologic map showing the geomorphic setting of the Arroyo del Valle Quarry area, based upon interpretation of stereo pairs of historic aerial photographs. The polygon in the upper left portion of the map shows the area of Figure 7.

setting of the southern Livermore Basin was shaped by fluvial deposition along Arroyo del Valle, a low-sinuosity (braided) stream. The stream channel is flanked by uplifts to the northeast and southwest. To the northeast, a subdued intrabasinal uplift is centered on the Livermore anticline that may be associated with a blind reverse or thrust fault (Sawyer and Unruh, 2004). To the southwest, tilted beds of the Livermore Formation flank the southwest margin of the basin. Between these two uplifts, Arroyo del Valle flows toward the northwest. A series of fluvial terraces ascend from the channel of Arroyo del Valle (youngest to oldest) and up the flanking uplifts northeast and southwest of the channel (Figure 3). The Arroyo del

Valle Quarry study area is located within the channel and adjacent alluvial terraces.

Site Stratigraphy

The quarry cut slopes expose only the shallowest portion of the basin stratigraphy. As a result of the lack of surface exposure, the primary tool for characterization of the deeper stratigraphy was subsurface exploration. Thus, 39 continuously cored borings and two large-diameter bucket auger borings were drilled for this study. The core samples were logged in detail, sedimentary characteristics were described, and marker beds were identified. Correlations between borings



Figure 4. Sandy gravel over a fine-grained bed exposed in the shallow portion of the quarry pit wall.

were added to detailed geologic cross sections, and structure contour maps were compiled using marker bed elevations.

Upper Sandy Gravel Deposits

The quarry pit slopes expose the upper sandy gravel deposits. These poorly sorted, coarse sediments consist of rounded to subangular cobbles, pebbles, and very coarse to fine sand with local boulders and minor low-plasticity silt and clay. Where exposed in quarry pit walls, local horizontal stratification and pebble imbrication are visible. Individual beds of sandy gravel have sharp, irregular lower contacts with well-developed erosional relief; this is particularly noticeable where the sandy gravel overlies local fine-grained beds (Figure 4). The sandy gravel unit varies in thickness from approximately 90 to 100 ft (27–30 m). The youngest gravel deposits exposed in the area of the historic stream channel are mostly gray, while older beds are oxidized to yellowish brown (Munsell color 10YR).

Interbedded with the sandy gravel are local beds of yellowish brown (10YR) clayey silt to silty clay that are generally less than 6 ft (2 m) in thickness (Figure 5). Based upon subsurface exploration, local fine-grained beds within the sandy gravel are mostly discontinuous, and where correlation of individual beds can be accomplished between boreholes, they appear to be horizontal or subhorizontal.

Lower Fine-Grained Deposits

In borings surrounding the quarry pit, fine-grained deposits were encountered below the upper sandy gravel deposits. The fine-grained strata consist of distinct beds of oxidized silty clay, unoxidized clay, marl, silty fine sand, and sandy silt. The oxidized



Figure 5. A fine-grained bed that pinches out laterally (exposed in the quarry pit wall).

clay displays variable coloration from light yellowish brown to strong brown (Munsell colors range from 2.5Y to 7.5YR). Though mostly lacking in stratification, the oxidized clay is locally laminated. The results of Atterberg Limits testing of the oxidized clay indicate that the average liquid limit and plasticity index are 37 and 15 (respectively), which correlate with low-plasticity clay. The color and texture of the oxidized clay strongly contrast with those of the underlying unoxidized clay.

The unoxidized clay is greenish gray to olive gray (5G to 5Y), with local lamination and significantly lower silt content (<10 percent silt) than the overlying oxidized clay. The results of laboratory testing of the unoxidized clay indicate that the average liquid limit and plasticity index are 75 and 48 (respectively), which places this clay in the high-plasticity range. In a few of the cores drilled northeast of the quarry pit, small pelecypod and gastropod shells and shell fragments were identified within the unoxidized clay. This stratigraphic unit displays evidence of intense shearing that includes numerous highly polished surfaces and development of clay gouge (Figure 6). The unoxidized clay overlies a white to light gray marl that is highly reactive to dilute hydrochloric acid. Below the marl is fine silty sand to sandy silt with interbedded silty clay; these strata are more permeable than the overlying unoxidized clay and marl.

The sheared, unoxidized clay and underlying marl form a distinctive and laterally persistent stratigraphic couplet. This couplet was traced across the quarry site and adjacent area to the northeast and is designated as the unoxidized clay-marl marker bed couplet.

Interpretation of Sedimentary Depositional Environments

Upper Sandy Gravel Deposits

The sandy gravel to gravelly sand encountered in the upper 100 ft (30 m) in the study area appears to



Figure 6. A core sample exposing a polished surface within the sheared unoxidized clay.

have been deposited in a braided stream environment similar to modern Arroyo del Valle. The predominantly coarse texture of this deposit is consistent with a high-velocity flow regime, and the horizontal stratification and pebble imbrication are consistent with deposition within a braided stream environment (Bridge and Lunt, 2006; Miall, 2010). Local discontinuous fine-grained beds within the upper sandy gravel were deposited at low flow velocity in an interchannel floodplain setting.

Lower Fine-Grained Deposits

The lower fine-grained deposits are interpreted as lacustrine sediments. The primary constituents are locally laminated clay with low silt content, marl, and silty clay. These sediments overlie silty fine sand and sandy silt. Though there is no single characteristic that defines a lacustrine depositional environment, typical indications include abundant fine-grained deposits, laterally continuous thin beds, lamination, freshwater fauna, organic-rich sediments, and evaporite or carbonate mineralogy (Picard and High, 1972, 1981; Platt and Wright, 1991; and Carroll and Bohacs, 1999). The laterally persistent fine-grained deposits, local lamination, carbonate-rich sediments, and local molluscan fauna of the lower fine-grained sedimentary strata are consistent with a lacustrine setting.

Interpretation of Geologic Structure and Stratigraphy

The study of geologic structure of the lower fine-grained strata has been greatly aided by the recognition of the unoxidized clay-marl marker bed couplet. Through detailed logging of core borings and careful

correlation of the marker bed couplet between these borings, structure contours were drawn on the top of the marker bed couplet (Figure 7). The structure contour map shows a northwest-plunging anticline in the northern portion of the study area and a northwest-plunging syncline in the southern portion. These folds align well with the orientation of other folds and thrust faults in the MDFTB. This implies that folding of the lacustrine sediments is related to northeast-southwest shortening within the MDFTB.

Though the lower fine-grained sedimentary deposits had not been recognized at the time of quarry excavation, the pit was excavated above the southwest-dipping limb of the anticline (Figure 7). A cross section across the quarry and northeast flank of the quarry shows the site stratigraphy and geologic structure (Figure 8). In the southwest limb of the anticline, the marker bed couplet strikes roughly 303° to 313° (N47W to N57W) and dips approximately 2° to the southwest. The dip of the northeast limb is approximately 4° to the northeast. By contrast, the overlying upper sandy gravel deposits do not appear to be folded. Based upon this angular discordance and the apparent truncation of the lower fine-grained strata in the northeastern portion of the study area, it appears that an unconformity separates the upper sandy gravel from the lower fine-grained deposits. Thus, we designate them as separate stratigraphic sequences. Though the exact ages of these two sequences is poorly constrained, based upon the topographic setting of these deposits and the contrast with the steeply tilted and folded Livermore Formation beds that are exposed in the nearby hills south of the basin, the lower fine-grained strata appear to be Pleistocene in age, and the upper sandy gravel strata appear to be late Pleistocene to Holocene in age.

HYDROGEOLOGY OF THE ARROYO DEL VALLE QUARRY AREA

Based upon subsurface exploration, three separate aquifers were identified at the Arroyo del Valle Quarry site. The shallowest aquifer is within the upper portion of the sandy gravel and above the discontinuous fine-grained beds. Below the discontinuous fine-grained beds is a semi-confined aquifer within the lower portion of the sandy gravel. The oxidized clay, unoxidized clay, and marl form an aquitard below the sandy gravel. The beds of sand and sandy silt below the unoxidized clay and marl constitute a confined aquifer. Within the study area, these three aquifer units are designated as the upper, middle, and lower aquifers (Figure 9). Though deeper aquifers may be present below the designated lower aquifer, this study did not include characterization of deeper aquifer stratigraphy.

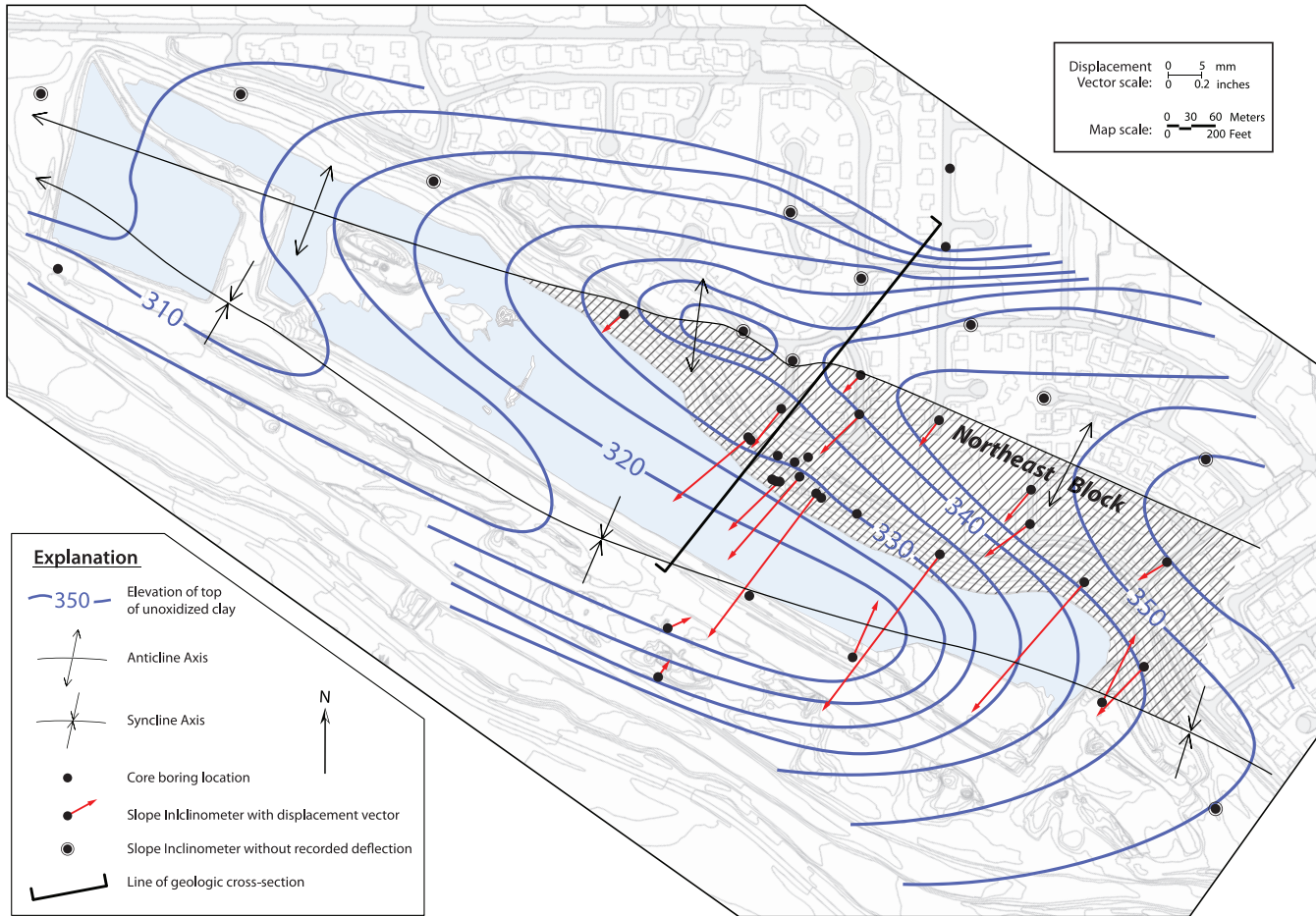


Figure 7. Site map with structure contours drawn on the top of the unoxidized clay-marl marker bed couplet. The cross-section line indicates the location of the geologic cross section (Figures 8, 9, and 13).

Long-term monitoring of vibrating wire piezometers installed in the lower aquifer indicates that piezometric surface elevations typically ranged from 75 to 102 ft (23–31 m) above the top of the lower aquifer. By contrast, the middle aquifer water levels have remained lower than those in the lower aquifer. Thus, the piezometer data indicate an upward gradient from the lower aquifer to the middle aquifer (Figure 9). Pore pressure measurements from piezometers installed in the unoxidized clay are intermediate between those of the middle and lower aquifers. This upward pore pressure gradient has caused elevated pore pressures within the intervening unoxidized clay interval.

SLOPE INSTABILITY

The instability of the quarry pit slopes is not readily apparent at the ground surface. As a result of the relatively small magnitude of displacement, roughly 4 to 5 in. (10–12 cm), typical landslide-related landforms (scarps, grabens, and hummocky topography) have not developed. The initial evidence for instability of

the quarry slopes came from linear cracks that formed in roadways located approximately 125 ft (38 m) northeast of the quarry pit (Figure 10). Following the initial observation of pavement distress in 2001, multiple slope inclinometers were installed around the quarry pit from 2002 to 2006.

Based upon detailed logging of continuous core samples from the slope inclinometer borings, discrete (landslide-type) deflections in the slope inclinometers were consistently found to correspond to the depth of the sheared unoxidized clay. This is shown in a data plot from a slope inclinometer located near the northeast flank of the quarry pit combined with the stratigraphic column from the same slope inclinometer boring (Figure 11). Even where the quarry pit walls were locally steeper than 2H:1V (26.6°), the slope inclinometer casings deflected only within the unoxidized clay and not within the upper sandy gravel sequence. Thus, the site stratigraphy exerts strong control on the instability of the quarry slopes.

Slope instability is also controlled by geologic structure. As shown in Figure 7, the slope inclinometer

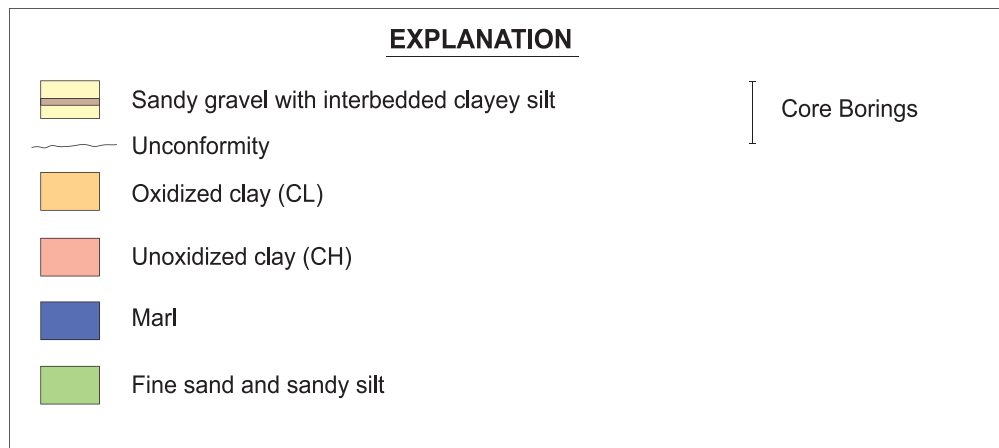
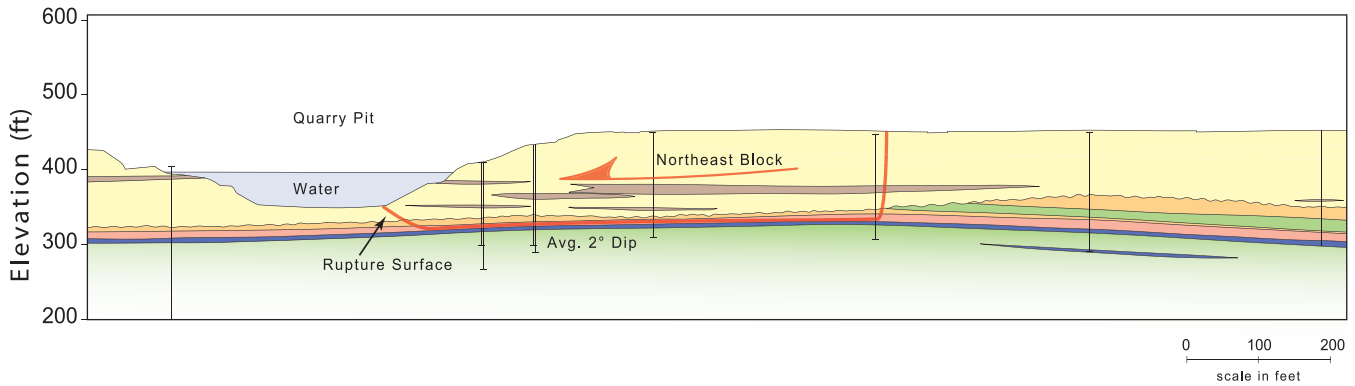


Figure 8. Geologic cross section across the quarry site and adjacent area northeast of the quarry.

displacement vectors are consistently oriented in a down-dip and downslope direction. At the northeast margin of the quarry, in the area between the anticline axis (Figure 7) and syncline that underlies the pit floor, slope inclinometer monitoring data show deflections in a down-dip direction, toward the pit. We refer to this critical sliding block where the sheared unoxidized clay dips toward the quarry pit as the Northeast Block. The anticline axis that forms the updip margin of the Northeast Block acts as a natural barrier to retrogressive movement farther to the northeast. Across the anticline axis, the sheared unoxidized clay bed dips away from the pit slope, and the slope inclinometers on this fold limb have not deflected.

The monitoring results from a representative slope inclinometer located on the upper bench on the northeast side of the quarry provide a useful record of displacement of the northeast block over a period of several years (Figure 12), although it does not include the estimated several inches of movement that occurred prior to slope inclinometer installation. For the purposes of this study, the rates of displacement were averaged and annualized to allow meaningful comparison of monitoring periods of varied durations. Between January 2004 and April 2005, slope

inclinometer monitoring results showed that the displacement rates averaged 0.26 in. (6.6 mm) per year. Between April and September of 2005, the displacement rate increased to an average of 1.0 in. (25.4 mm) per year. Between September 2005 and September 2006, an average displacement rate of 0.14 in. (3.5 mm) per year was recorded. Thus, prior to implementation of mitigation measures designed to address slope instability at the quarry pit, the rate of movement within the Northeast Block had already slowed.

The recent displacement that occurred on the northeast flank of the quarry pit would be insufficient in magnitude to produce the well-developed polished

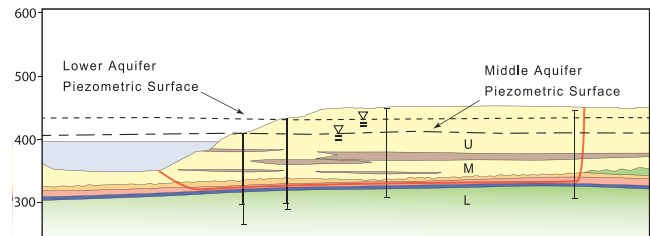


Figure 9. Hydrogeologic cross section showing the piezometric surfaces of the middle and lower aquifers within the Northeast Block. U, upper aquifer; M, middle aquifer; L, lower aquifer.

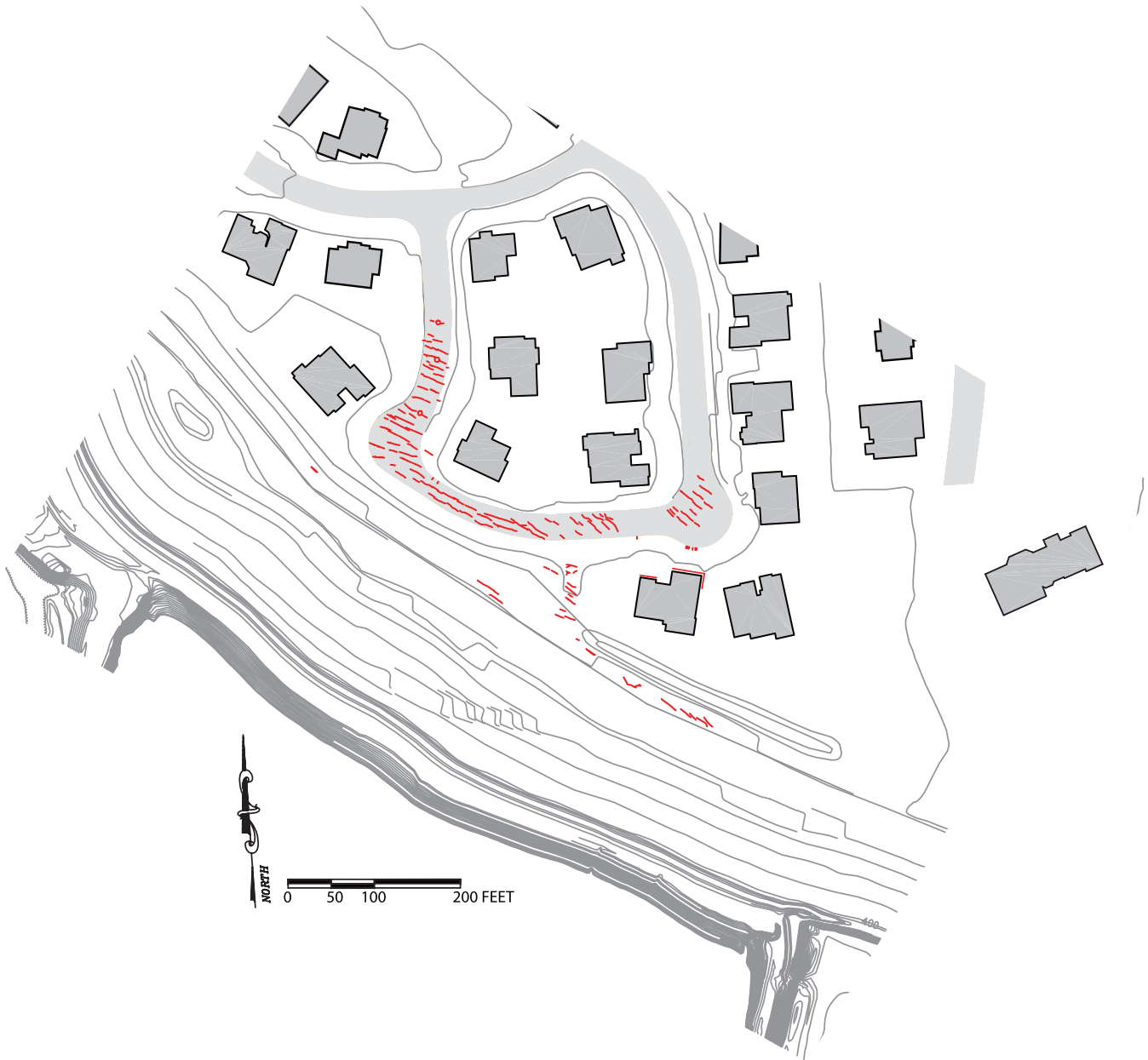


Figure 10. Map of ground cracks that were the first indication of incipient slope instability related to the quarry pit slope.

surfaces and clay gouge observed in the unoxidized clay. In addition, the unoxidized clay was encountered in an intensely sheared state in borings throughout the study area, including the fold limb that dips away from the quarry pit. Therefore, it appears that the unoxidized clay was sheared prior to excavation of the quarry pit.

Based upon the slope inclinometer data, it is clear that the inclinometer deflections were a response to stress release and removal of lateral confinement due to quarry pit excavation. This stress release triggered downslope movement in the weak unoxidized clay bed where it dips toward the quarry pit excavation.

The high pore-water pressures within the unoxidized clay also contributed to instability of the Northeast Block. The movement of the Northeast Block that followed pit excavation appears to represent incipient landsliding because it did not develop into a larger magnitude failure.

GEOTECHNICAL ANALYSIS AND DESIGN OF MITIGATION MEASURES

Limit equilibrium and finite element slope stability analyses were performed to assess the instability and factor of safety (FS) of the Northeast Block. The

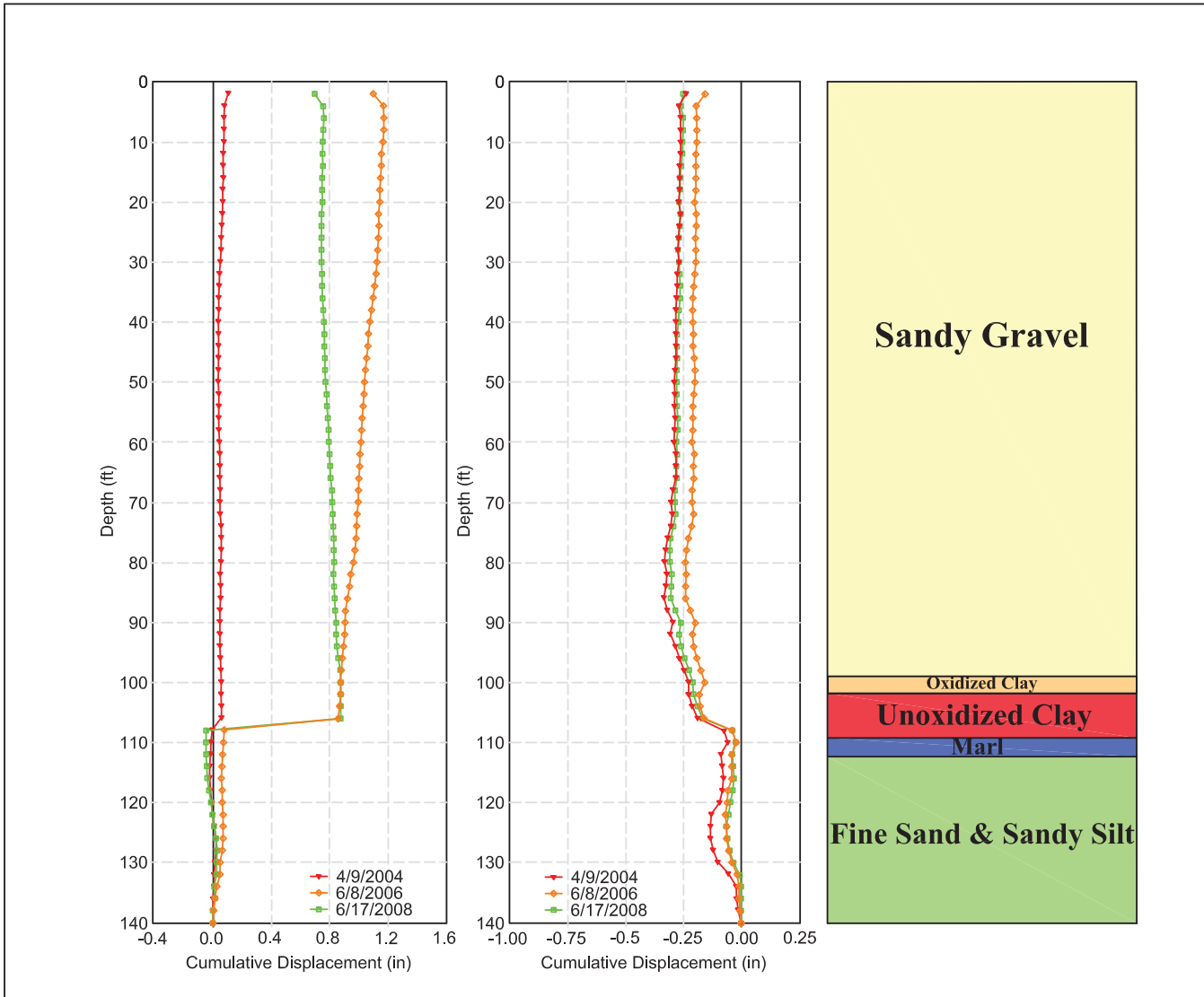


Figure 11. Slope inclinometer data plot and stratigraphic column from a slope inclinometer located near the northeast flank of the quarry pit.

analyses indicated that the shear strength of the sandy gravel was incrementally mobilized as displacements occurred within the sheared unoxidized clay. This explains the decline in slope inclinometer deflection over time. Under static conditions, the slopes should experience little displacement once the gravel strength has been fully mobilized. However, under seismic conditions, the Northeast Block would be expected to reactivate, potentially leading to much larger displacements. Consequently, implementation of mitigation measures was necessary to provide for the long-term stability of the Northeast Block during future seismic events.

Though several methods of mitigation were considered, an earth-fill buttress repair was chosen for its simplicity and reliability. Limit equilibrium slope stability analyses showed that the pressure exerted by

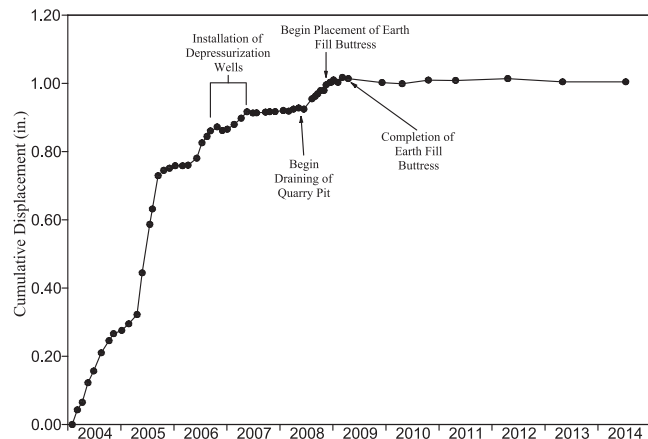


Figure 12. Graph of cumulative displacement over time at the unoxidized clay interval from a representative slope inclinometer on the northeast flank of the quarry pit.

water within the quarry pit acted to resist movement of the Northeast Block. If the pit were drained to allow placement of an earth-fill buttress, displacements within the Northeast Block would likely accelerate until the gravel strength was fully mobilized. Thus, mitigation measures designed to stabilize the Northeast Block had to maintain short-term stability during placement of the buttress.

A two-dimensional limit equilibrium slope stability analysis was performed on a representative cross section using Spencer's method (Wright, 1975) to evaluate the stability of the Northeast Block during placement of the buttress and to calculate the potential seismic displacements after completion of the buttress. The key parameters for this slope stability analysis included topographic profile, rupture surface geometry, material shear strengths, unit weights, and piezometric surface elevations. The material shear strengths were determined by laboratory testing (consolidated-undrained triaxial compression and torsional ring shear testing) and back-calculation analyses. The shear strengths for the sandy gravels in particular were difficult to estimate because of difficulties in obtaining undisturbed samples of the sandy gravel material for triaxial shear strength testing due to the large clast size. Therefore, in addition to triaxial compression testing, back-calculation analyses of the sandy gravel material strengths were performed on areas of the quarry where the sandy gravel was exposed in near-vertical cut faces of approximately 35 ft in height. Several small failures had occurred in these cut faces, and based on these analyses the laboratory-derived peak shear strength was actually lower than the back-calculated shear strengths. Correlations between gravel particle size and friction angle were also considered in developing the shear strengths. Based on these sources, representative shear strengths for the sandy gravel material were selected as shown in Table 1. The material unit weights were determined by laboratory testing of undisturbed samples. The shear strengths and unit weights are compiled in Table 1. The topographic profile and subsurface geometry were taken from a representative geologic cross section (Figure 8), and the piezometric surface elevations were derived from monitoring of piezometers within the study area.

In addition to the stratigraphic units previously described, two additional materials were placed as fill for the earth-fill buttress: ½-in.- (13-mm-) diameter pea gravel and compacted pit run fill. The pea gravel was produced by processing of material excavated from one of the other nearby gravel quarries. The pit run material consisted of sandy gravel excavated from a borrow area at the southwest margin of the

Table 1. Summary of static material properties.

Material	Unit Weight (pcf)	Cohesion (psf)	Friction Angle (°)
Sandy gravel	139	200	45
Clay beds within sandy gravel	127	1,500	27
Oxidized clay	130	1,000	24
Sheared unoxidized clay	121	0	11
Unoxidized clay gouge (residual shear strength)	121	0	Non-linear (~6)
Lower confined aquifer	133	1,300	28
Compacted pea gravel fill	134	0	Non-linear (~40 to 51)
Compacted pit run fill	145	100	39

quarry pit and placed as engineered fill without additional processing.

The piezometric surface elevations were determined by long-term monitoring of staged vibrating wire piezometers that were installed within the Northeast Block and elsewhere around the study area. The piezometer sensors were divided into three groups: "upper sensors," "mid-sensors," or "lower sensors," based on the aquifer stratigraphy and depth of sensor placement (Figure 9). The upper aquifer and discontinuous fine-grained beds within the gravel were assigned the "upper sensor" piezometric surface. The middle aquifer was assigned the "mid-sensor" piezometric surface. The unoxidized clay and lower aquifer were assigned the "lower sensor" piezometric surface. For design of the buttress, the highest recorded levels for each sensor group were used to estimate the piezometric surface for each hydro-stratigraphic unit.

The initial analyses indicated that the calculated FS values ranged from 1.22 to 1.70 (depending on the rupture surface analyzed) using peak shear strengths for most materials and residual shear strength for rupture surface gouge, as shown in Table 1. The unexpected finding that FS remained above 1.0 while active landslide-type movement was apparently underway is best explained by the high strength of the sandy gravel material. The slope movement response to the quarry excavation was concentrated on the unoxidized clay, while the relatively strong sandy gravel near the toe of the slope provided shearing resistance to this deep movement in the unoxidized clay. Because the amount of movement in the unoxidized clay was relatively small, displacement did not reach the point at which the peak shear strength of the sandy gravel near the toe of the slope was fully mobilized. Therefore, when using peak strength values for the sandy gravel in the slope stability analyses, the overall static FS of the slope (including the impact of the resisting sandy gravel) remained above unity, although local discrete

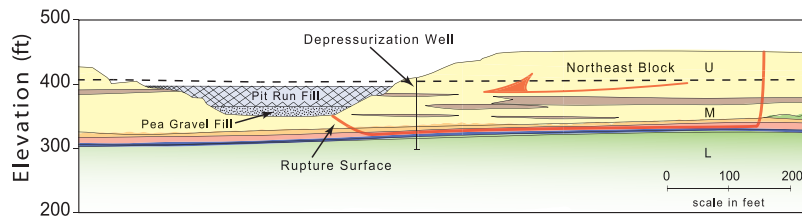


Figure 13. The geologic cross section annotated to show the phases of grading during placement of the earth-fill buttress. The depressurization wells are screened in the lower aquifer. U, upper aquifer; M, middle aquifer; L, lower aquifer. The dashed horizontal line represents the elevation of the lower aquifer piezometric surface after installation of the depressurization wells.

shearing movement in the unoxidized clay occurred in response to the excavation. Once sufficient displacement within the unoxidized clay had occurred, the shearing resistance of the sandy gravel was partially mobilized, and displacement within the unoxidized clay slowed. These analyses expose an oversimplifying assumption typically used for limit equilibrium slope stability analysis, that the FS is uniform along all portions of the rupture surface analyzed whether the rupture surface passes through weak clay at residual strength or strong gravel with no previous history of shearing.

In addition to the static slope stability analyses that were conducted, seismic displacements were also estimated using a Newmark-type sliding block analysis (Jibson and Jibson, 2003). Three active faults (the Calaveras, Greenville, and Hayward faults, located 9.3 to 19.1 km from the site) were identified as most likely to affect the site, with moment magnitudes ranging from 6.6 to 7.1. A design target response spectrum was developed for the site based upon multiple attenuation relationships with modifications for near-fault effects. Seven strong motion records (Pacific Earthquake Engineering Research Center, 2000) were selected that were representative of the expected ground motion at the site and scaled as necessary to obtain a relatively close fit between the average response spectrum of the seven motions and the target design response spectrum. One-dimensional equivalent-linear seismic response analysis (SHAKE2000, 2000) was performed on three representative stratigraphic columns to obtain horizontal equivalent acceleration time histories at the depth of sliding, which were then used in conjunction with yield accelerations from pseudo-static slope stability analyses to estimate seismic displacements (Koragappa et al., 2004).

Based upon these analyses, the movement of the Northeast Block resulted from stress relief upon excavation of the free face at the northeast margin of the quarry pit. The previously sheared clay that was at or near residual shear strength prior to quarry pit excavation and the elevated pore pressures within the critical sliding surface were the primary factors resulting in the movement detected initially as ground cracks in

nearby roads and later by the slope inclinometers. Using partially mobilized upper gravel strengths, piezometric influence from the lower aquifer, and potential movement that extends northeastward to the anticline axis, our analysis showed that an industry-accepted static FS of greater than 1.5 and seismic displacements of less than 15 cm (6 in.) could be achieved by partial filling of the quarry pit with engineered fill to an elevation of 390 ft (119 m) above sea level (Figure 13).

IMPLEMENTATION OF MITIGATION MEASURES

Between September 2006 and May 2007, 40 depressurization wells were installed on the northeast flank of the quarry to relieve pore-water pressures within the lower aquifer. Based upon the site hydrogeology, lowering of the piezometric surface within the lower aquifer was expected to reduce pore pressures within the overlying unoxidized clay and, in turn, to improve the static FS of the Northeast Block. Immediately upon installation, the depressurization wells flowed at the surface under artesian conditions. As anticipated, the artesian flow resulted in lowering of the piezometric surface of the lower aquifer to roughly the elevation of the well discharge pipes. The piezometric surface at a representative piezometer within the Northeast Block (Figure 14) shows this initial drop. Following installation of the depressurization wells, the displacement rates in slope inclinometer SI-2 decreased to an average of 0.04 in. (1 mm) per year between September 2006 and May 2008 (Figure 12). During May 2008, submersible pumps with float-activated controllers were installed in 10 of the wells. Within 9 days of pump activation, the elevation of the piezometric surface within the lower aquifer (Figure 14) had dropped by 43 ft (13 m). Within 3 months after pump activation, the piezometric surface elevation had dropped an additional 20 ft (6 m).

Following activation of the well pumps and prior to placement of the fill buttress, the quarry pit (artificial lake) was partially drained. Between June 2008 and August 2008, the water surface elevation of the lake

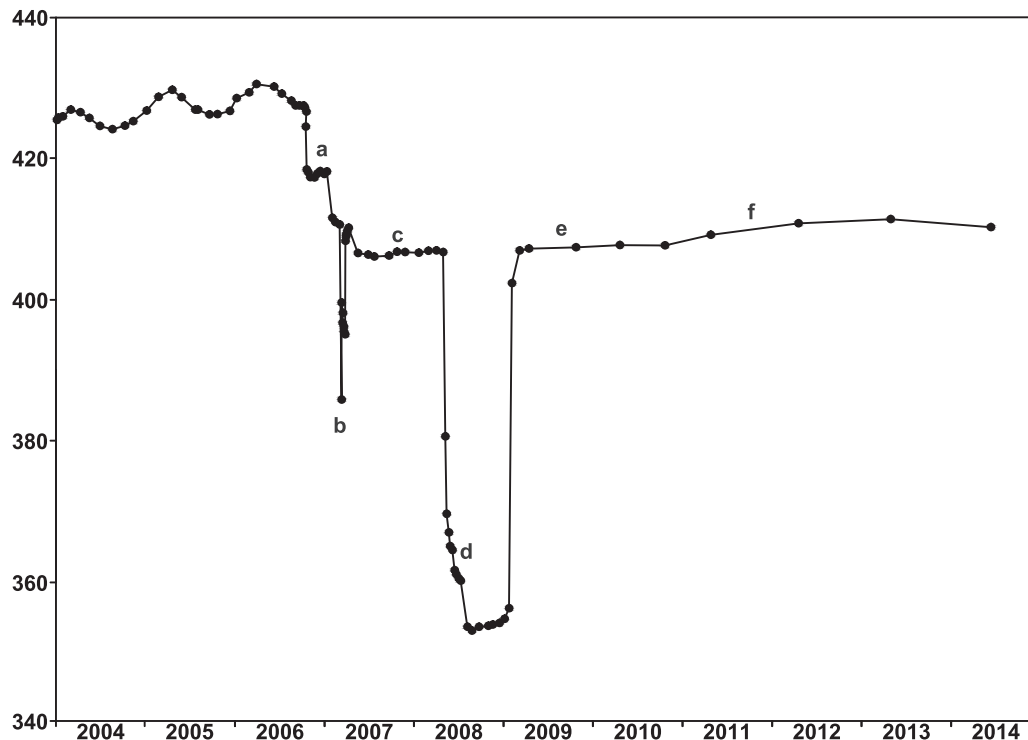


Figure 14. Piezometric surface elevation data from a representative piezometer installed in the confined lower aquifer on the northeast side of the quarry pit. (a) Initial drop in piezometric surface during installation of depressurization wells; (b) brief pumping test on a single depressurization well; (c) well discharge to the quarry pit maintains a constant piezometric surface elevation of approximately 407 ft (the elevation of the well discharge lines); (d) significant lowering of the piezometric surface during pumping of 10 depressurization wells; (e) return to equilibrium conditions following cessation of well pumping; (f) slight rise of the piezometric surface as the lake surface elevation increased and the well discharge lines were inundated.

was lowered approximately 13 ft (4 m) by pumping. During this period of time, some slope inclinometers within the Northeast Block showed a modest acceleration in deflection rate. Between June 2008 and November 2008, the average slope inclinometer displacement rate was 0.18 in. (4.5 mm) per year (Figure 12). Thus, even partial draining of the lake did affect slope stability, as predicted.

In order to temporarily stabilize the Northeast Block before the quarry pit was fully drained, a temporary buttress was placed on the lake bottom. The temporary buttress consisted of pea gravel fill that was dropped through the water column and onto the lake bottom using a floating conveyor belt system. Figure 13 shows the buttress in cross-section view. Prior to construction, analysis of the loose dumped pea gravel fill indicated that it could be susceptible to liquefaction associated with strong seismic ground motions, so it was necessary to compact the pea gravel fill to provide long-term stability under future seismic loading conditions. Once the lake was drained and the pea gravel fill could be dewatered, it was excavated in slots oriented perpendicular to the slope and not more than 100 ft (30 m) wide in order to preserve the buttressing effect. The pea gravel was placed back

into the slots in lifts and compacted to 95 percent relative compaction. After recompaction was completed, the elevation of the top of the pea gravel fill was 364.5 ft (111.1 m).

Following placement and recompaction of the pea gravel fill, drainage of the pit continued, and pit run material was excavated from a shallow borrow area southwest of the pit and placed as compacted fill over the pea gravel using conventional grading methods. As placement of the fill buttress progressed, the slope inclinometer displacement rate slowed to 0.045 in. (0.11 mm) per year between November 2008 and April 2009. The completed fill buttress reached the final elevation of 390 ft (118.9 m) during April 2009. Subsequent monitoring of site slope inclinometers and piezometers from 2009 through 2014 has shown no evidence of an increased rate of movement (Figure 12) even though the piezometric surface of the lower aquifer has risen since pumping of the depressurization wells ceased (Figure 14).

CONCLUSIONS

The unique stratigraphy, geologic structure, and hydrogeology at the Arroyo del Valle Quarry site

and surrounding area were key factors that led to incipient failure of the northeast slope of the quarry pit (the Northeast Block). The highly sheared unoxidized clay found in the subsurface was weakened to residual shear strength by other geologic processes prior to excavation of the quarry pit, and this very low shear strength made it vulnerable to instability once the quarry pit was excavated. The slope inclinometers deflected only within the unoxidized clay interval; thus, the site stratigraphy strongly controlled incipient landslide movement. Slope inclinometer displacements occurred only where the unoxidized clay dips toward the quarry pit. Therefore, geologic structure also controlled incipient landsliding. Elevated pore-water pressures within the unoxidized clay appear to be related to the high pore pressures within the underlying lower aquifer and the upward hydraulic gradient between the lower and middle aquifers. Thus, the site hydrogeology also contributed to the instability of the Northeast Block.

Based upon our analyses, we conclude that incipient landsliding resulted from the site geologic and hydrogeologic conditions described above combined with stress relief related to excavation of the quarry pit. Initial deflection within the weak unoxidized clay eventually led to partial mobilization of the strength of the overlying gravel and a decline in slope inclinometer deflection rate. However, the static FS remained below the industry-accepted minimum value of 1.5, and unacceptably large displacements were anticipated under seismic loading conditions. Thus, it was necessary to design and implement mitigation measures to address the static and seismic stability of the Northeast Block.

Because the pressure exerted by the water that filled the former quarry pit provided some counterbalance to the forces driving slope movement, the lake could not be drained without triggering significant acceleration in slope movement. Initially, the pore pressures within the unoxidized clay were lowered using depressurization wells screened in the lower aquifer combined with pumping of those wells. Then a temporary buttress of pea gravel was placed on the floor of the former quarry pit before the lake was completely drained. Once drained, the pea gravel was removed in slots, compacted as it was placed back into the slots, and capped with additional engineered fill that was placed using conventional grading methods.

Limit equilibrium analyses show that the completed buttress should provide a FS of greater than 1.5 under static conditions, even as pore pressures within the unoxidized clay rise. Displacements that could result from strong seismic shaking were calculated at less than 6 in. (15 cm) with the earth-fill buttress in place.

Five years of post-construction monitoring have shown no evidence of renewed slope inclinometer deflection within the Northeast Block or elsewhere around the quarry site.

ACKNOWLEDGMENTS

This project was completed with the review, assistance, and guidance of professors Jonathan Bray, Scott Kiefer, and Matthew Mauldon. Geotechnical laboratory testing was provided by Cooper Testing Labs, Inc. The authors wish to thank Dale Marcum, Joe Durdella, Jason Nichols, Jonathan Sleeper, Jamie Smith, and many others at Cotton Shires and Associates, Inc., for their assistance during completion of this project. We wish to thank Michael Hart, Douglas M. Yadon, and an anonymous reviewer for their helpful comments that improved this manuscript.

REFERENCES

- ANDERSEN, D. W.; ISAACSON, K. A.; AND BARLOCK, V. E., 1995, Neogene evolution of the Livermore Basin within the California Coast Ranges. In Fritsche, A. E. (Editor), *Cenozoic Paleogeography of the Western United States II*: Pacific Section SEPM Publication 75, pp. 151–161.
- BARLOCK, V., 1989, *Sedimentology of the Livermore Gravels (Miocene-Pleistocene)*, Southern Livermore Valley, California: U.S. Geological Survey Open File Report 89-131, 93 p.
- BRIDGE, J. S. AND LUNT, I. A., 2006, Depositional models of braided rivers. In Sambrook Smith, G. H.; Best, J. L.; Bristow, C. S.; and Petts, G. E. (Editors), *Braided Rivers*: International Association of Sedimentologists Special Publication No. 36, pp. 11–50.
- CALIFORNIA DEPARTMENT OF WATER RESOURCES (CDWR), 1974, *Evaluation of Groundwater Resources, Livermore and Sunol Valleys*: CDWR Bulletin 118-2, 153 p.
- CARROLL, A. R. AND BOHACS, K. M., 1999, Stratigraphic classification of ancient lakes: Balancing tectonic and climatic controls: *Geology*, Vol. 27, No. 2, pp. 99–102.
- CRANE, R., 1995, Geology of the Mount Diablo region and East Bay hills. In Sangines, E. M.; Andersen, D. W.; and Buising, A. V. (Editors), *Recent Geologic Studies in the San Francisco Bay Area*: Pacific Section SEPM Special Publication, Vol. 76, pp. 87–114.
- CRANE, R., 2007, *Geology of Central California*: Pacific Section American Association of Petroleum Geologists, CD-ROM No. 4, 237 p.
- DOUGHTON, S., 2009, State warned gravel pit of slope instability 4 years before landslide: *Seattle Times*, October 16, 2009.
- DUPRAS, D., 1999, Representative industrial mineral mines of the San Francisco Bay region: Sand and gravel, crushed rock, and limestone. In Wagner, D. L. and Graham, S. A. (Editors), *Geologic Field Trips in Northern California*: California Division of Mines and Geology Special Publication 119, pp. 235–245.
- EHMAN, K. D.; FIGUERS, S.; AND BLAKE, R., 2004, Preliminary stratigraphic evaluation, west side of the main basin, Livermore-Amador groundwater basin: unpublished consultant's report to Zone 7 Water Agency, 25 p.

- GOLDMAN, H. B., 1964, *Sand and Gravel in California, and Inventory of Deposits, Part B Central California*: California Division of Mines and Geology Bulletin 180-B, 58 p.
- HELLEY, E. J. AND GRAYMER, R. W., 1997, *Quaternary Geology of Alameda County and Surrounding Areas, California*: U.S. Geological Survey Open File Report 97-97, 1:100,000 scale.
- HOEK, E. AND KARZULOVIC, A., 2000, Rock mass properties for surface mines. In Hurstrulid, W. A.; McCarter, M. K.; and Van Zyl, D. J. A. (Editors), *Slope Stability in Surface Mining*: SME, Littleton, CO, pp. 59–70.
- JIBSON, R. W. AND JIBSON, M. W., 2003, *Java Programs for Using Newmark's Method and Simplified Decoupled Analysis to Model Slope Performance During Earthquakes*: U.S. Geological Survey, Open File Report 2003-005, CD-ROM.
- KORAGAPPA, N.; BRAY, J. D.; MEYER, D.; AND TRAVASAROU, T., 2004, Seismic slope stability of a landfill on young bay mud: *Proceedings Waste Tech Landfill Technology Conference*, Dallas, TX, May 17–19, 2004, 22 p.
- MIALL, A., 2010, Alluvial deposits. In James, N. P. and Dalrymple, R. W. (Editors), *Facies Models 4*: Geological Society of Canada, GEOText 6, pP. 105137.
- PACIFIC EARTHQUAKE ENGINEERING RESEARCH CENTER, 2000, *Ground Motion Database*: Electronic document, available at <http://peer.berkeley.edu>
- PANKOW, K. L.; MOORE, J. R.; HALE, J. M.; KOPER, K. D.; KUBACKI, T.; WHIDDEN, K. M.; AND MCCARTER, M. K., 2014, Massive landslide at Utah copper mine generates wealth of geophysical data: *GSA Today*, Vol. 24, pp. 4–9.
- PICARD, M. D. AND HIGH, L. R., 1972, Criteria for recognizing lacustrine rocks. In Rigby, J. K. and Hamblin, W. K. (Editors), *Recognition of Ancient Sedimentary Environments*: SEPM Special Publication, No. 16, pp. 108–145.
- PICARD, M. D. AND HIGH, L. R., 1981, Physical stratigraphy of ancient lacustrine deposits. In Ethridge, F. G. and Flores, R. M. (Editors), *Recent and Ancient Nonmarine Depositional Environments*: SEPM Special Publication, No. 31, pp. 108–145.
- PLATT, N. H. AND WRIGHT, V. P., 1991, Lacustrine carbonates: Facies models, facies distributions and hydrocarbon aspects. In Anadon, P.; Cabrera, L.; and Kelts, K. (Editors), *Lacustrine Facies Analysis*: International Association of Sedimentologists Special Publication, No. 13, pp. 57–74.
- SAWYER, T. L. AND UNRUH, J. R., 2004, *Characterization of Late Quaternary Deformation of the Mt. Diablo Fold-and-Thrust Belt, Eastern San Francisco Bay Area, California*: EOS Transactions, Vol. 85, Fall Meeting Supplement, Abstract T32C-02.
- SHAKE2000, 2000, *A Computer Program for the 1-D Analysis of Geotechnical Earthquake Engineering Problems*: Gustavo A. Ordonez, GeoMotions, LLC, Lacy, WA.
- UNRUH, J. R.; DUMITRU, T. A.; AND SAWYER, T. L., 2007, Coupling of early Tertiary extension in the Great Valley forearc with blueschist exhumation in the underlying Franciscan accretionary wedge at Mount Diablo, California: *Geological Society America Bulletin*, Vol. 119, pp. 1347–1367.
- UNRUH, J. R. AND LETTIS, W. R., 1998, Kinematics of compressional deformation in the eastern San Francisco Bay region, California: *Geology*, Vol. 26, pp. 19–22.
- UNRUH, J. R.; SAWYER, T. L.; KNUDSEN, K. L.; AND LETTIS, W. R., 1997, *Assessment of Blind Seismogenic Sources, Livermore Valley, Eastern San Francisco Bay Region, Final Technical Report*: U.S. Geological Survey NEHRP Award No. 1434-95-G-2611, 88 p.
- WAGNER, D. L.; BORTUGNO, E. J.; AND MCJUNKIN, R. D., 1990, *Geologic Map of the San Francisco–San Jose Quadrangle*: California Division of Mines and Geology, Regional Geologic Map Series, Map No. 5A, 5 sheets, 1:250,000.
- WRIGHT, S. G., 1975, *Evaluation of Slope Stability Procedures*: American Society of Civil Engineers, preprint 2616, National Convention, Denver, CO, 28 p.
- WYLLIE, D. C. AND MAH, C. W., 2004, *Rock Slope Engineering: Civil and Mining*: Taylor & Francis, New York, NY, 456 p.